

# Numerical Studies of Straw Tube Detectors

---

**R. Kanishka**

*Department of Physics, University Institute of Sciences, Chandigarh University, Mohali, Punjab, India 140413.*

*E-mail:* [kanishka.rawat.phy@gmail.com](mailto:kanishka.rawat.phy@gmail.com)

**ABSTRACT:** The charged particles are tracked in the high energy physics detectors to provide the information of their properties. One of the tracking detector is straw tube detector that has been used by many experiments. The aim of this paper is to study the different properties of particles using different gas composition. The gas mixture that shows maximum transition radiation among xenon gas mixtures was found to be  $XeHeCH_4 :: 30:55:15$ . The gas mixture that has shown maximum primary ionization has been  $XeCO_2O_2 :: 70:27:3$ . The simulated detector has been also used for the identification of different particles.

**KEYWORDS:** Gaseous detectors, Wire chambers, Ionization and excitation processes, Transition radiation detectors

---

## Contents

<b>1</b>	<b>Introduction</b>	<b>1</b>
<b>2</b>	<b>Numerical Studies with Different Gases</b>	<b>2</b>
<b>3</b>	<b>Results</b>	<b>2</b>
3.1	<sup>60</sup> CO Decay	2
3.2	Performance of Straw Tube Detectors using Different Particles	6
<b>4</b>	<b>Summary and Conclusions</b>	<b>8</b>

---

## 1 Introduction

The gaseous detectors have been used by many particle physics experiments. Their applications require to optimize the gaseous detector itself whether its the optimization of detector geometries and/or gas mixtures. To understand the performance of the detector simulations can be of great help. The straw tube detectors are used by many ongoing and upcoming particle physics experiments to track the different particles. The COMPASS [1], PANDA [2]–[4], ATLAS [5]–[10], NA62[11], GlueX[12] and an upcoming experiment like DUNE [13]–[14] have been using the straw tube trackers (STT) [15]. Each of these experiments have different physics goals and hence the different geometries and, composition of gas mixtures. There are numerous characteristics of straw tube detectors like the excellent vertex, momentum, angular, and time resolution that makes them special for doing several studies.

The current work aims to do different numerical studies to check the performance of the straw tube detectors. The primary ionization is crucial in the high rate experiments for charge density and discharge studies [16]. These discharges if not detected damages the detector and makes them non-operational and hence repairing the detectors again would be time consuming and costly. In another work, the detector was chosen to study X-ray transition radiation (XTR) [17] which is caused when a charged particle passes through the boundary between two materials with different dielectric constants. The multiple foils interleaved with air in the current simulated detector has been capable of detecting the XTRs. In this paper the particle identification has also been done by simulating the different particles namely, electrons, muons, pions and muons. The detector is also capable to detect beta decay of <sup>60</sup>CO as have been discussed in this paper.

This paper has been organized as follows: section 2 describes numerical studies with different gas mixtures. The results have been discussed in the section 3. The summary and conclusions have been discussed in the end in the section 4.

## 2 Numerical Studies with Different Gases

The detector has been simulated with geant4 toolkit [18] and the data was further analyzed using ROOT software [19]. The simulated detector has been capable of nuclear reactions as well as particle detection. The set up consists of graphite layer and the radiators that are made of polypropylene foils. These foils have the 18  $\mu\text{m}$  thickness and 117  $\mu\text{m}$  air gap between them. The straw tubes are placed across x-y plane which are made up of mylar and the inner wire is made up of 95% tungsten and 5% gold. These straw tubes are filled with gas mixtures as mentioned in this section. Table 1 shows the dimensions of the detector that have been taken for analysis:

**Table 1.** The dimensions of the detector.

Dimensions of graphite target	1m $\times$ 1m $\times$ 0.004m
Dimensions of polypropylene foils	1m $\times$ 1m $\times$ 3cm
No. of Straw tubes	100
Straw tube inner radius	2.5 mm
Straw tube outer radius	3.5 mm
Wire inner radius	5 $\mu\text{m}$
Wire outer radius	10 $\mu\text{m}$
Length of wire	900 mm

The choice of gases has been done by choosing the base components of the TR gas mixture i.e., xenon with its excellent X-ray absorption in combination with the different quenchers. Also, xenon shows the maximum ionization among other noble gases [20]. The optimization of gas mixtures with different ratios has been done to check the performance of straw tube detectors. The mixture of gases at STP with different compositions have been used for the analysis. These compositions are:  $XeCO_2O_2::70:27:3$  [21]–[22],  $XeCO_2N_2::70:27:3$ ,  $XeHeCH_4::30:55:15$  [23],  $XeCO_2::70:30$  [24],  $XeCH_4::70:30$  [25],  $XeC_5H_{12}::70:30$  [26].

## 3 Results

10,000 different particles i.e.,  $^{60}\text{CO}$  source, pions, kaons, muons, electrons were shot in the z-direction in the detector for further analysis.

### 3.1 $^{60}\text{CO}$ Decay

The detector was irradiated with a gamma source  $^{60}\text{CO}$  for detecting the beta decay [27]. The physics lists for  $^{60}\text{CO}$  decay were, GammaNuclearPhysics and G4DecayPhysics. The figure 1 shows the geant4 display for straw tube detectors irradiated with  $^{60}\text{CO}$ . The  $^{60}\text{CO}$  source passes through graphite and transition radiators and deposit their energy in  $ArCO_2$  which was taken in the ratio of 70:30. The  $^{60}\text{CO}$  undergoes beta decay as shown in eq. (3.1) and have a half-life of 5.272 years. The  $^{60}\text{CO}$  decay scheme has been shown in the figure 2. The figure 3 shows the  $^{60}\text{CO}$  decay in straw tube detectors. The two peaks at 1.1 and 1.3 MeV shows the  $^{60}\text{CO}$  decay into a stable  $^{60}\text{Ni}$  as per the decay scheme shown in figure 2.

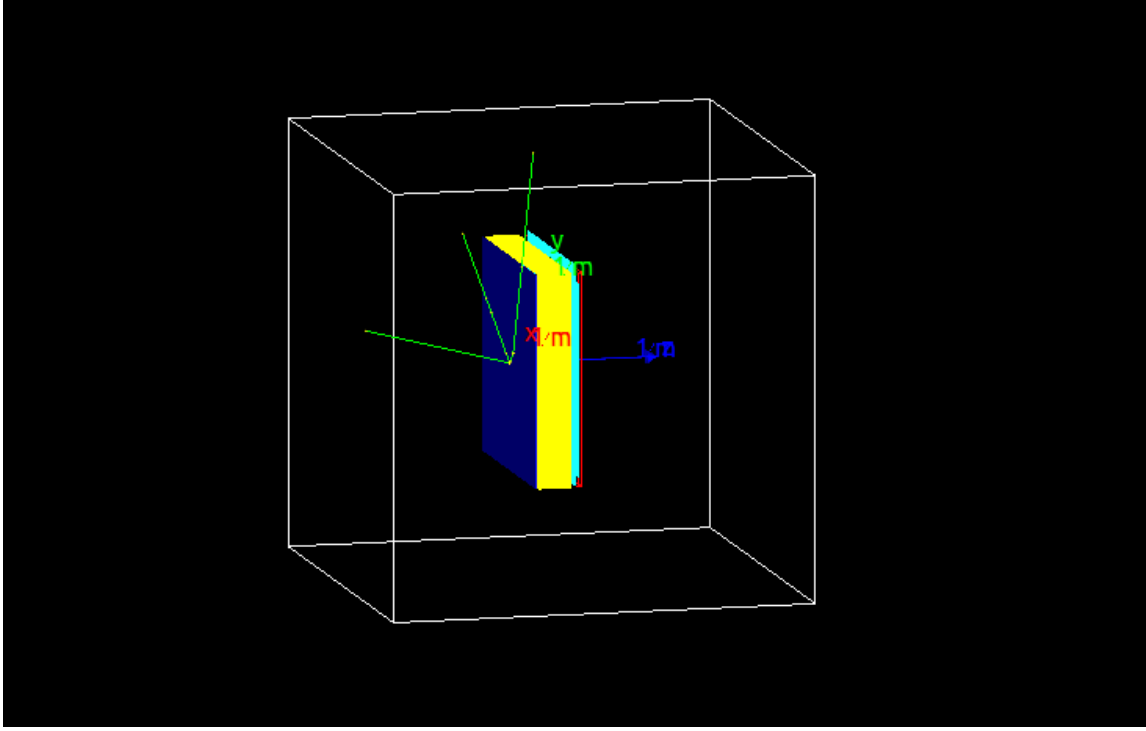


**Figure 1.** The geant4 display for straw tube detectors irradiated with CO-60. Note: The blue plate represents graphite plate, yellow plates represents transition radiation detectors, cyan tubes represents straw tubes along x- and y- directions both, red box represents gas volume, white box represents world volume. The green colour particles are gamma and yellow points are hits.

X-ray transition radiation (XTR) photons are released when a relativistic particle traverses an inhomogeneous medium i.e., through the boundary between materials of different electrical properties [28]–[32]. The geant4 G4StrawTubeXTRadiator model was chosen to obtain the XTR photons. Figure 4 shows the XTR photon yield as a function of the Lorentz factor for different gas mixtures. The figure shows that as Lorentz factor increases the XTR yield also increases and gets saturated at the Lorentz factor of 46520 as XTR yield saturates with the multiple foils. Among all the gas mixtures as mentioned in the section 2,  $\text{XeHeCH}_4 :: 30:55:15$  shows the highest XTR yield due to the highest mobility of XTR photons in the low density of helium. Figure 5 shows the XTR gamma spectrum for different gas mixtures, as discussed the  $\text{XeHeCH}_4 :: 30:55:15$  shows the highest number of XTR photons.

The different gas mixtures have been analyzed to obtain primaries and the spatial distributions [33]. 10,000 electrons of 1 GeV were shot from  $x=0$  cm,  $y=0$  cm,  $z=0$  cm in the six gas mixtures as discussed in section 2. The electrons were shot along z-direction. The physics list chosen for the interactions was G4EmStandardPhysics. The figure 6 shows the x-, y- and z- distributions of electrons in different gas mixtures. The primary ionization has been obtained highest in the

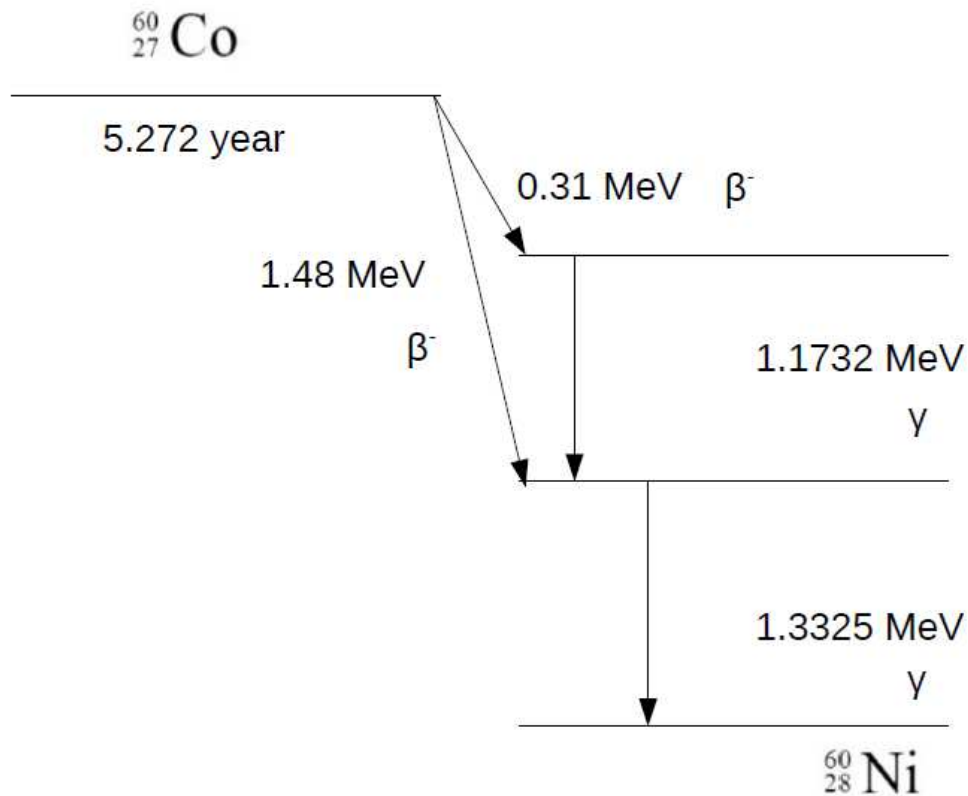


**Figure 2.** The decay scheme of  ${}^{60}\text{Co}$  into  ${}^{60}\text{Ni}$ .

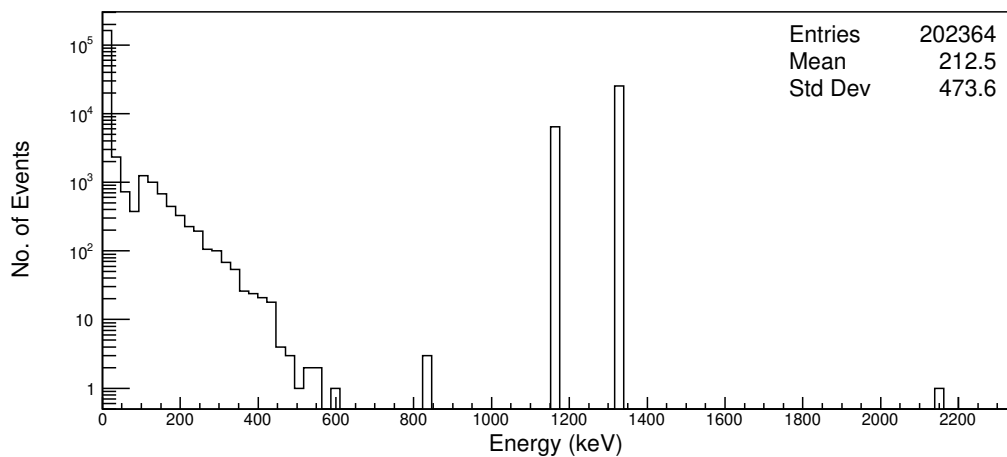


**Figure 3.** The figure shows the Cobalt decay in straw tube detectors. The two peaks show the Cobalt decay at 1.1 and 1.3 MeV.

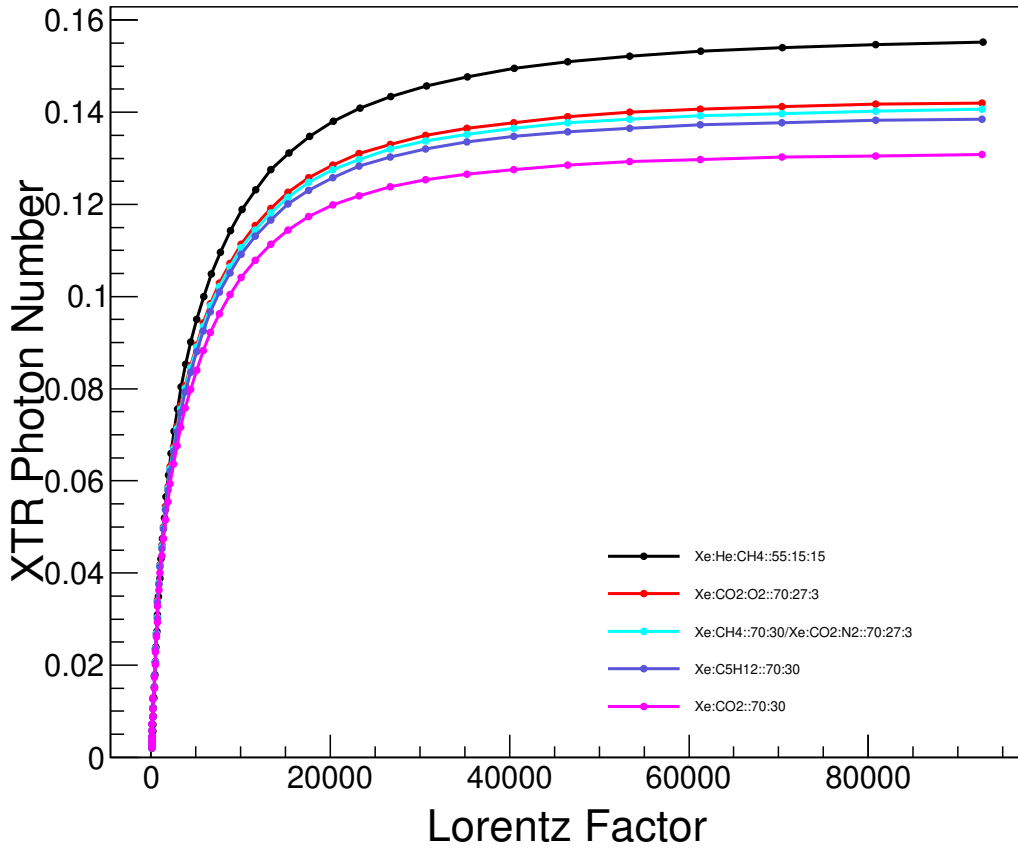


Figure 4. XTR photon number as a function of the Lorentz factor for different gas mixtures.

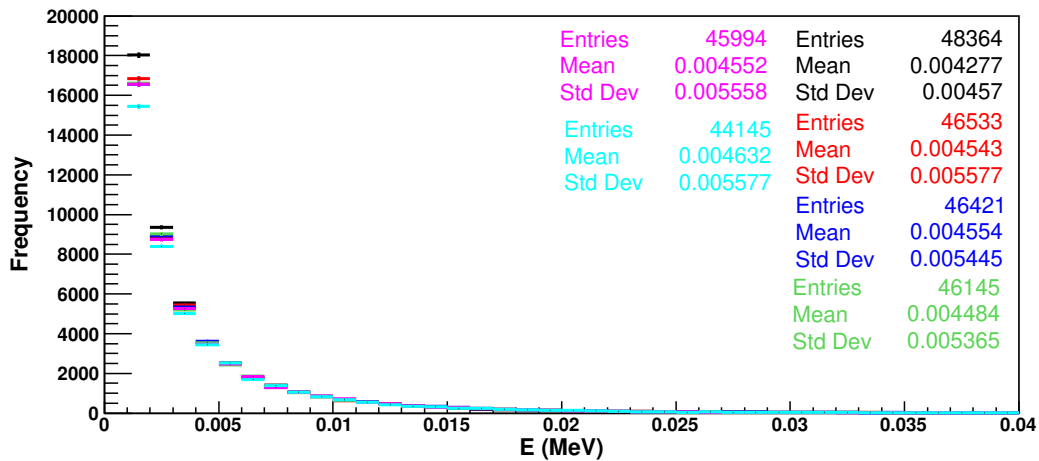


Figure 5. The XTR gamma spectrum as a function of energy for different gas mixtures. Note that, the colour scheme for different gases are: black -  $XeHeCH_4$ , red -  $XeCO_2O_2$ , blue -  $XeCH_4$ , green -  $XeCO_2N_2$ , pink -  $XeC_5H_{12}$ , cyan -  $XeCO_2$ .

$XeCO_2O_2$  gas mixture. The figure also shows the Gaussian distributions due to large statistics. The deviation from zero is due to the particles were shot along the negative z-direction. The electrons were shot along negative z direction shows the z- distribution started from -2000 mm to till it was stopped in the gas. The figure 7 shows the view of x- and y- distributions in 2-dimensions. The center part shows that the particles were shot from  $x=0$  cm,  $y=0$  cm. The figure 8 shows the energy loss by primaries and secondaries when 10000 electrons of 1 GeV were shot in the gas mixture  $XeCO_2O_2 :: 70:27:3$ . The table 2 shows the primaries in different gas mixtures, that have been separated from secondaries which is required to do charge density studies in many high energy physics experiments.

**Table 2.** The number of primaries for different gas mixtures.

Gases	Composition	No. of primaries
$XeCO_2O_2$	70:27:3	635172
$XeCO_2N_2$	70:27:3	630775
$XeHeCH_4$	30:55:15	629548
$XeCO_2$	70:30	626554
$XeC_5H_{12}$	70:30	625360
$XeCH_4$	70:30	624823

### 3.2 Performance of Straw Tube Detectors using Different Particles

The detector was also studied for its performance using different particles. 10,000 pions were shot in the different gas mixtures. The physics lists chosen for the analysis were, G4HadronElasticPhysicsHP and G4HadronPhysicsFTFP\_BERT\_HP. The figure 9 shows the kinetic energy distribution of pions for different gas mixtures. The plot shows the peak at 1 GeV which is due to pions shot at the same energy of 1 GeV. The pions were further analyzed in the  $XeCO_2O_2 :: 70:27:3$  gas mixture, since it shows maximum ionization. The pions ( $\pi^-$ ) that decays into muons ( $\mu^-$ ) have been identified [34]–[43] in the gas mixture and has been shown in figure 10.

Another particle that was chosen were muons. 10,000 muons have been shot in the gas mixture  $XeCO_2O_2 :: 70:27:3$  for their identification. The physics list for the interactions include G4EmStandardPhysics. The figure 11 shows the muons that have been decayed into electrons in the same gas mixture have been identified.

The next particle chosen to be identified were kaons. 10,000 kaons were shot in the geant4 toolkit. The physics lists were chosen to be same as that of pions. The kaons and its decay products have been identified in the detector as shown in figure 12. Kaon decays into several products as shown in the eq. (3.2). These particles deposited their energies in the straw tube detector that has been shown in figure. The kaon decays into  $mu^-$ ,  $pi^-$  mainly,  $mu^-$  further decays into  $e^-$  that has been shown in the figure.

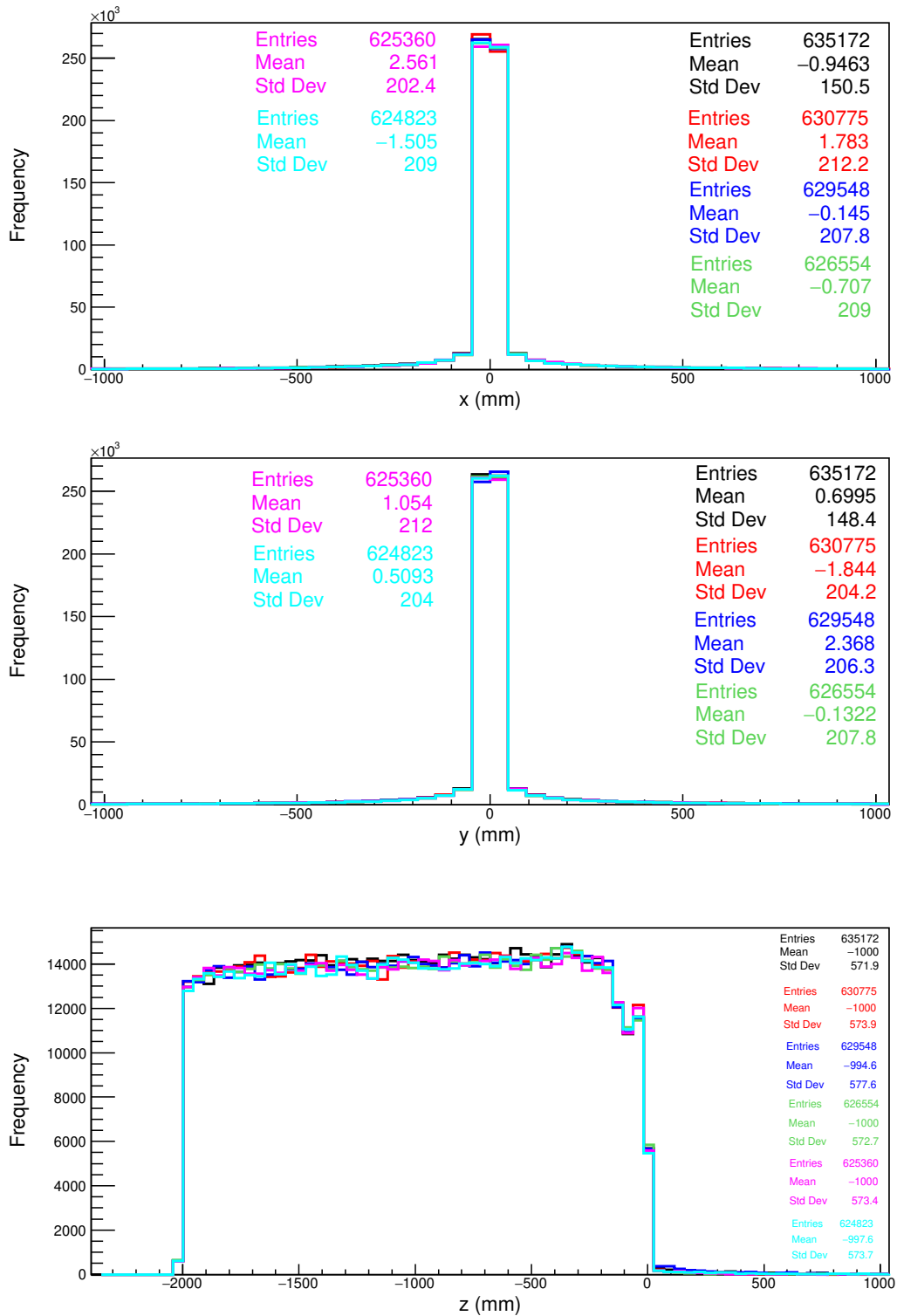


**Figure 6.** The x-, y- and z- distributions of the primary ionizations when electrons of 1 GeV were shot. Note that, the colour scheme for different gases are: black -  $XeCO_2O_2$ , red -  $XeCO_2N_2$ , blue -  $XeHeCH_4$ , green -  $XeCO_2$ , pink -  $XeC_5H_{12}$ , cyan -  $XeCH_4$ .

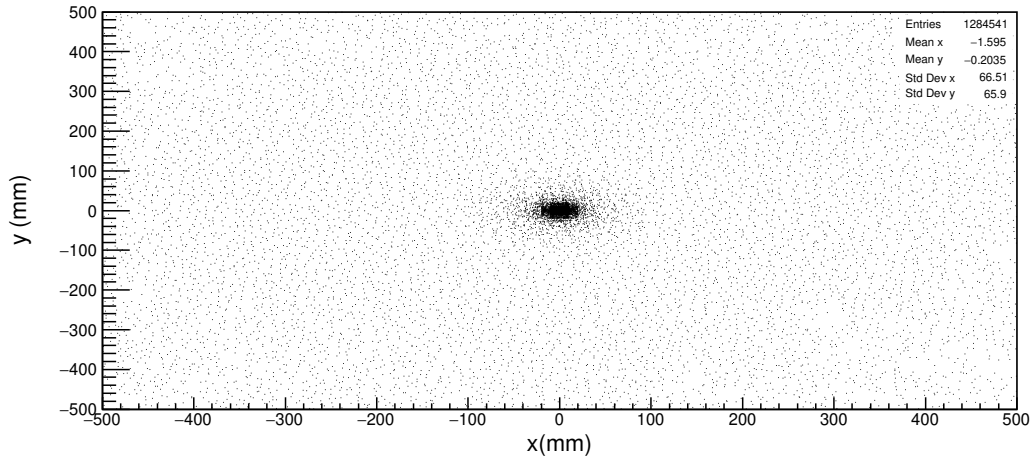


**Figure 7.** The figure shows the variation of x- and y- coordinates in 2 dimensions.

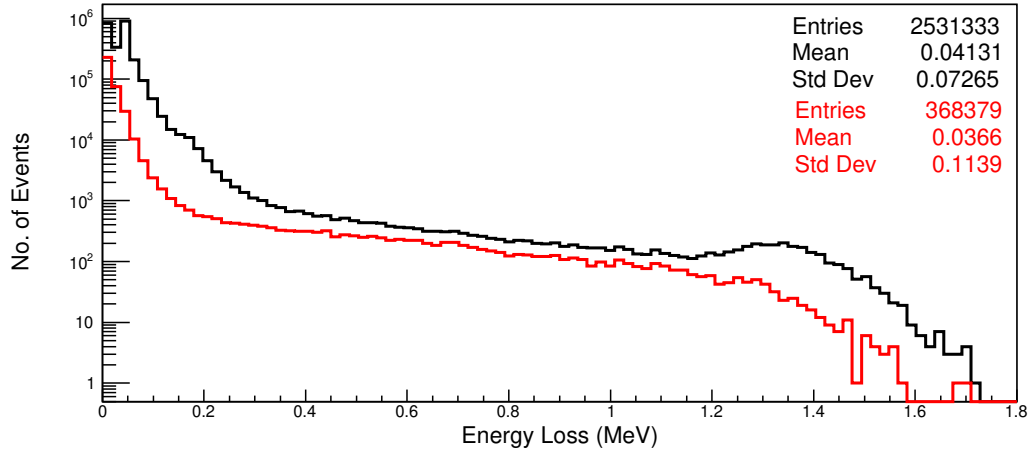


**Figure 8.** The energy loss of primaries (black) and secondaries (red) when electrons of 1 GeV were shot in the gas  $XeCO_2O_2 :: 70:27:3$ .

$$K^- \rightarrow \mu^- + \bar{\nu}_\mu \quad (3.2)$$

$$K^- \rightarrow \pi^- + \pi^0 \quad (3.3)$$

$$K^- \rightarrow \pi^0 + \mu^- + \bar{\nu}_\mu \quad (3.4)$$

$$\mu^- \rightarrow e^- + \bar{\nu}_e \quad (3.5)$$

## 4 Summary and Conclusions

Straw tube detectors are a type of particle detectors commonly used in high-energy physics experiments to track charged particles. They consist of thin-walled, gas-filled tubes (often made of a

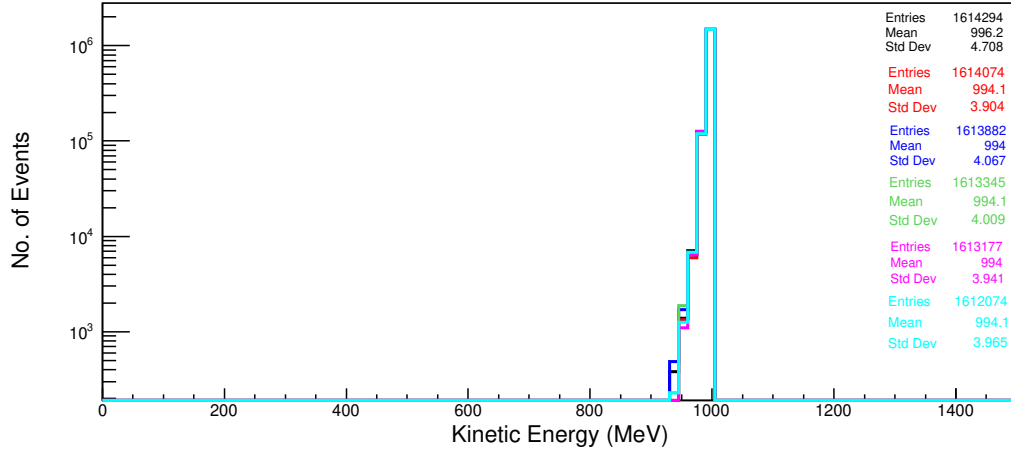


**Figure 9.** The distribution of kinetic energy of pions of 1 GeV for the different gas mixtures. Note that, the colour scheme for different gases are: black -  $XeCO_2O_2$ , red -  $XeCO_2$ , blue -  $XeHeCH_4$ , green -  $XeC_5H_{12}$ , pink -  $XeCH_4$ , cyan -  $XeCO_2N_2$ .

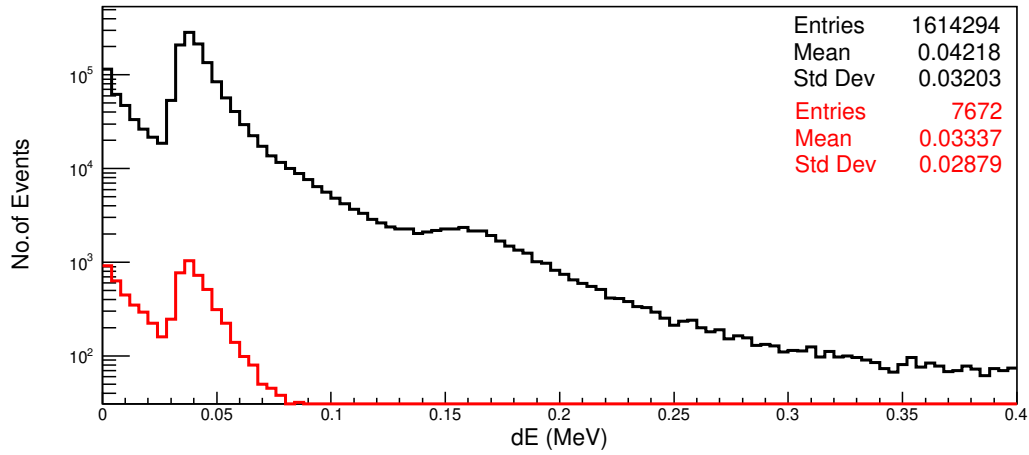


**Figure 10.** Figure shows the energy deposition distribution of pions and its decayed products when pions of 1 GeV were shot in the gas  $XeCO_2O_2 :: 70:27:3$ . Note that, the color scheme for different decay products are: black -  $\pi^-$ , red -  $\mu^-$ .

lightweight material) with a wire running along the central axis. When a charged particle passes through the tube, it ionizes the gas inside, creating free electrons and ions. The central wire, held at a high voltage, attracts the electrons, causing a measurable current. Straw tube detectors have wide range of applications due to their high precision, low mass and modularity.

The present paper evaluates the numerical studies using different gas mixtures. The presented simulated detector is suitable for both nuclear physics reactions and particle physics studies. The energy spectrum from the simulation of  $^{60}Co$  into  $^{60}Ni$  have shown the two  $^{60}Ni$  peaks of 1.1 and 1.3 MeV. The different gas mixtures using different compositions i.e.,  $XeCO_2O_2::70:27:3$ ,

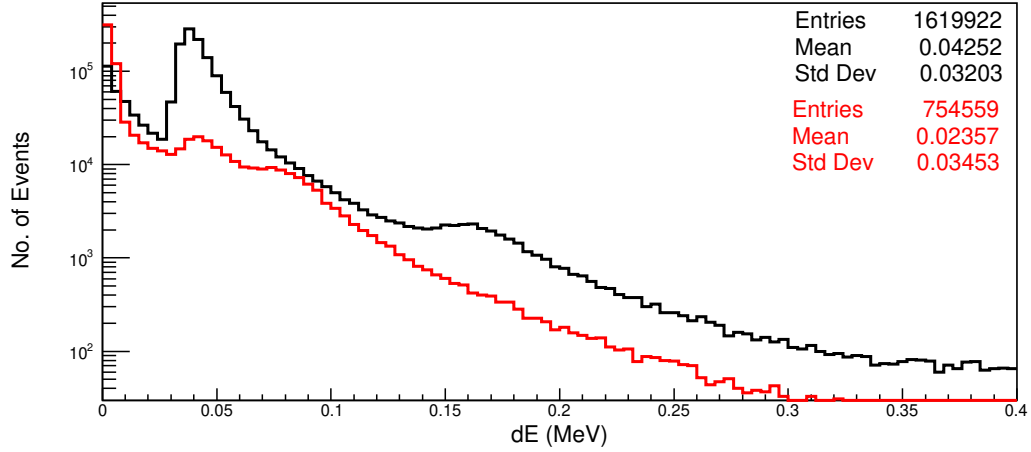


**Figure 11.** The energy deposition distribution of muons (black) and its decayed products, electrons (red), when muons of 1 GeV were shot in the gas  $XeCO_2O_2 :: 70:27:3$ .

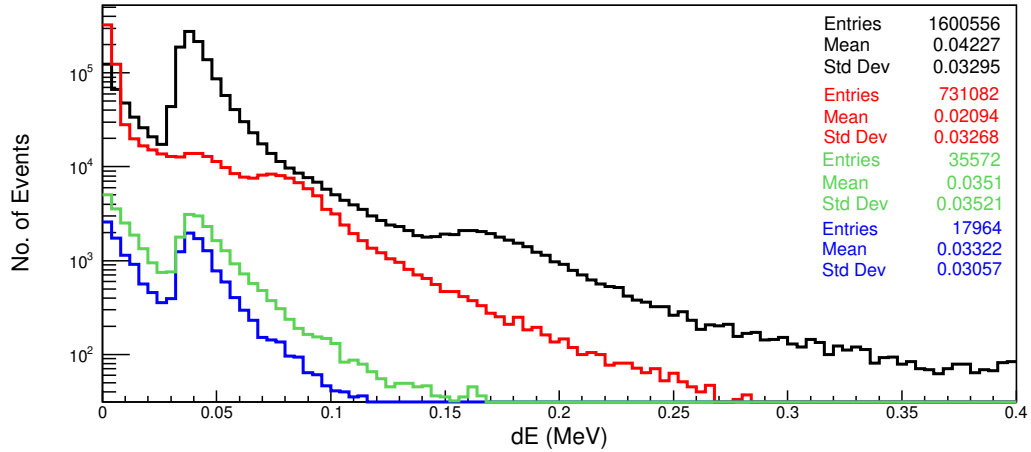


**Figure 12.** The figure shows the energy deposition distribution of kaons and its decayed products when kaons of 1 GeV were shot in the gas  $XeCO_2O_2 :: 70:27:3$ . Note that, the color scheme for different decay products are: black - kaons, red - electrons, green -  $\mu^-$ , blue -  $\pi^-$ .

$XeCO_2N_2::70:27:3$ ,  $XeHeCH_4::30:55:15$ ,  $XeCO_2::70:30$ ,  $XeCH_4::70:30$ ,  $XeC_5H_{12}::70:30$  have been utilized for XTR photon production and primaries. The XTR yield [44]–[45] was found to be highest in the  $XeHeCH_4::30:55:15$  gas mixture and the number of primaries were maximum in  $XeCO_2O_2::70:27:3$  gas mixture. The different particles i.e., muons, pions and kaons have been shot in the detector that have been decayed into their respective products. These particles and their products have been identified in the detector. These studies can be useful for the future particle physics experiments to check the performance of their detectors.

## Acknowledgments

I would like to thank the department of physics, Chandigarh University for help and support.

## References

- [1] V. N. Bychkov et. al., *The large size straw drift chambers of the COMPASS experiment*, *NIM A* **556** (1) (2006) 66-79. <https://doi.org/10.1016/j.nima.2005.10.026>
- [2] P. Gianotti et al., *The straw tube trackers of the PANDA experiment*, *3<sup>rd</sup> International Conference on Advancements in Nuclear Instrumentation, Measurement Methods and their Applications (ANIMMA)*, Marseille, France (2013) 1–7. <https://doi.org/10.1109/ANIMMA.2013.6728039>
- [3] J. Smyrski et. al., *Design of the forward straw tube tracker for the PANDA experiment*, *JINST* **12** (2017) C06032. <https://doi.org/10.1088/1748-0221/12/06/C06032>
- [4] P. Wintz, *For the PANDA Tracking Group, The central straw tube tracker in the PANDA experiment*, *Hyperfine Interactions* **229** (2014) 147–152. <https://doi.org/10.1007/s10751-014-1035-6>
- [5] T. Akesson et.al., *Straw tube drift-time properties and electronics parameters for the ATLAS TRT detector*, *NIM A* **449** (3) (2000) 446–460. [https://doi.org/10.1016/S0168-9002\(99\)01470-9](https://doi.org/10.1016/S0168-9002(99)01470-9)
- [6] Ahmet Bingul, *The ATLAS TRT and its Performance at LHC*, *J. Phys.: Conf. Ser.* **347** (2012) 012025. <https://doi.org/10.1088/1742-6596/347/1/012025>
- [7] Abat E. et al., *The ATLAS TRT collaboration, The ATLAS Transition Radiation Tracker (TRT) proportional drift-tube: Design and Performance*, *JINST* **3** (2008) P02013. <https://doi.org/10.1088/1748-0221/3/02/P02013>
- [8] Abat E. et al., *The ATLAS TRT collaboration, The ATLAS TRT Barrel Detector*, *JINST* **3** (2008) P02014. <https://doi.org/10.1088/1748-0221/3/02/P02014>
- [9] Abat E. et al., *The ATLAS TRT collaboration, The ATLAS TRT end-cap detectors*, *JINST* **3** (2008) P10003. <https://doi.org/10.1088/1748-0221/3/10/P10003>
- [10] Abat E. et al., *The ATLAS TRT collaboration, The ATLAS TRT electronics*, *JINST* **3** (2008) P06007. <https://doi.org/10.1088/1748-0221/3/06/P06007>
- [11] A. Sergi, *NA62 Spectrometer: A Low Mass Straw Tracker*, *Physics Procedia* **37** (2012) 530–534. <https://doi.org/10.1016/j.phpro.2012.03.713>
- [12] N. S. Jarvis et. al., *The Central Drift Chamber for GlueX*. *United States: N. p.* **962** (2020) 163727. <https://doi.org/10.1016/j.nima.2020.163727>
- [13] B. Abi et. al., *Volume I. Introduction to DUNE*, *JINST* **15** (2020) T08008. <https://doi.org/10.1088/1748-0221/15/08/T08008>
- [14] A. A. Abud et. al., *Deep Underground Neutrino Experiment (DUNE) Near Detector Conceptual Design Report*, *Instruments* **5**(4) (2021) 31. <https://doi.org/10.3390/instruments5040031>
- [15] T. Akesson et. al., *Study of straw proportional tubes for a transition radiation detector/tracker at LHC*, *NIMA* **361** (3) (1995) 440–456. [https://doi.org/10.1016/0168-9002\(95\)00075-5](https://doi.org/10.1016/0168-9002(95)00075-5)
- [16] P. K. Rout, R. Kanishka et. al., *Numerical estimation of discharge probability in GEM-based detectors*, *JINST* **16** (2021) P09001. [10.1088/1748-0221/16/09/P09001](https://doi.org/10.1088/1748-0221/16/09/P09001)
- [17] T. Akesson et. al., *ATLAS TRT collaboration, Electron identification with a prototype of the Transition Radiation Tracker for the ATLAS experiment*, *NIMA* **412** (2–3) (1998) 200–215. [https://doi.org/10.1016/S0168-9002\(98\)00457-4](https://doi.org/10.1016/S0168-9002(98)00457-4)

- [18] S. Agostinelli et al., *Geant4-a simulation toolkit*, *NIMA* **506**, (2003)250. <https://geant4.web.cern.ch/>
- [19] <https://root.cern/>.
- [20] A. Andronic, J. P. Wessels, *Transition radiation detectors*, *NIMA* **666** (2012) 130–147. <https://doi.org/10.1016/j.nima.2011.09.041>
- [21] Adrian Vogel, *For ATLAS Collaboration, ATLAS Transition Radiation Tracker (TRT): Straw tube gaseous detectors at high rates*, *NIMA* **732** (2013) 277–280. <https://doi.org/10.1016/j.nima.2013.07.020>
- [22] Bartosz Mindur, *For ATLAS Collaboration, ATLAS Transition Radiation Tracker (TRT): Straw tubes for tracking and particle identification at the Large Hadron Collider*, *NIMA* **845** (2017) 257–261. <https://doi.org/10.1016/j.nima.2016.04.026>
- [23] G. D. Barr et. al., *A large-area transition radiation detector*, *NIMA* **294**(3) (1990) 465–472 [https://doi.org/10.1016/0168-9002\(90\)90287-G](https://doi.org/10.1016/0168-9002(90)90287-G)
- [24] K. Aamodt et. al., *For The ALICE Collaboration, The ALICE experiment at the CERN LHC*, *JINST* **3** (2008) S08002. <https://doi.org/10.1088/1748-0221/3/08/S08002>
- [25] B. Libby et. al., *Particle identification in TEC/TRD Prototypes for the PHENIX detector at RHIC*, *NIMA* **367**(1–3) (1995) 244–247. [https://doi.org/10.1016/0168-9002\(95\)00646-X](https://doi.org/10.1016/0168-9002(95)00646-X)
- [26] Boris Dolgoshein, *Transition radiation detectors*, *NIMA* **326**(3) (1993) 434–469. [https://doi.org/10.1016/0168-9002\(93\)90846-A](https://doi.org/10.1016/0168-9002(93)90846-A)
- [27] P. Rice-Evans and Z. Aung, *On the decay of cobalt 60*, *Z. Physik* **240** (1970) 392–395. <https://doi.org/10.1007/BF01395575>
- [28] M. L. Cherry et. al., *Transition radiation from relativistic electrons in periodic radiators*, *Phys. Rev. D* **10**(11) (1974) 3594–3607. <https://doi.org/10.1103/PhysRevD.10.3594>
- [29] X. Artru et. al., *Practical theory of the multilayered transition radiation detector*, *Phys. Rev. D* **12** (1975) 1289–1306. <https://doi.org/10.1103/PhysRevD.12.1289>
- [30] L. Durand, *Transition radiation from ultrarelativistic particles*, *Phys. Rev. D* **11**(1) (1975) 89–105. <https://doi.org/10.1103/PhysRevD.11.89>
- [31] E. Barbarito et. al., *A large area transition radiation detector to measure the energy of muons in the Gran Sasso underground laboratory*, *NIMA* **365**(1) (1995) 214–223 [https://doi.org/10.1016/0168-9002\(95\)00475-0](https://doi.org/10.1016/0168-9002(95)00475-0)
- [32] J. Gu et. al., *The photon yield efficiency study of transition radiators at E2 line of Beijing Test Beam Facility*, *JINST* **16** (2021) P08041 <https://doi.org/10.1088/1748-0221/16/08/P08041>
- [33] R. Kanishka, S. Mukhopadhyay, N. Majumdar, S. Sarkar, *A Simulation of Primary Ionization for Different Gas Mixtures*, *Springer Proc. Phys.* **282** (2023) 47–53. [https://doi.org/10.1007/978-3-031-19268-5\\_6](https://doi.org/10.1007/978-3-031-19268-5_6)
- [34] C. W. Fabjan, W. Struczinski, *Coherent emission of transition radiation in periodic radiators*, *Phys. Lett. B* **57**(5) (1975) 483–486. [https://doi.org/10.1016/0370-2693\(75\)90274-9](https://doi.org/10.1016/0370-2693(75)90274-9)
- [35] C. Camps et al., *Transition Radiation from Electrons at Low gamma Values*, *Nucl. Instr. and Meth.* **131**(3) (1975) 411–416. [https://doi.org/10.1016/0029-554X\(75\)90426-7](https://doi.org/10.1016/0029-554X(75)90426-7)
- [36] J. Cobb et. al., *Transition Radiators for electron Identification at the CERN ISR*, *Nucl. Instr. and Meth.* **140**(3) (1977) 413–427. [https://doi.org/10.1016/0029-554X\(77\)90355-X](https://doi.org/10.1016/0029-554X(77)90355-X)

- [37] C. W. Fabjan et. al., *Transition Radiation Spectra from Randomly Spaced Interfaces*, *Nucl. Instr. and Meth.* **146**(2) (1977) 343–346. [https://doi.org/10.1016/0029-554X\(77\)90718-2](https://doi.org/10.1016/0029-554X(77)90718-2)
- [38] M. L. Cherry et. al., *Measurements of the spectrum and energy dependence of x-ray transition radiation*, *Phys. Rev. D* **17** (1978) 2245. <https://doi.org/10.1103/PhysRevD.17.2245>
- [39] C. W. Fabjan et. al., *Practical Prototype of a Cluster Counting Transition Radiation Detector*, *Nucl. Instr. and Meth.* **185**(1–3) (1981) 119–124. [https://doi.org/10.1016/0029-554X\(81\)91202-7](https://doi.org/10.1016/0029-554X(81)91202-7)
- [40] A. Bungener et. al., *ELECTRON IDENTIFICATION BEYOND 1-GEV BY MEANS OF TRANSITION RADIATION*, *Nucl. Instr. and Meth.* **214**(2–3) (1983) 261–268. [https://doi.org/10.1016/0167-5087\(83\)90592-6](https://doi.org/10.1016/0167-5087(83)90592-6)
- [41] R. D. Appuhn et. al., *Transition Radiation Detectors for Electron Identification Beyond 1-GeV/c*, *NIMA* **263**(2–3) (1988) 309–318 [https://doi.org/10.1016/0168-9002\(88\)90965-5](https://doi.org/10.1016/0168-9002(88)90965-5)
- [42] V. Commichau et. al., *A transition radiation detector for pion identification in the 100 GeV/c momentum region*, *Nuclear Instruments and Methods* **176**(1–2) (1980) 325–331. [https://doi.org/10.1016/0029-554X\(80\)90724-7](https://doi.org/10.1016/0029-554X(80)90724-7)
- [43] M. Deutschmann et. al., *Particle identification using the angular distribution of transition radiation*, *Nuclear Instruments and Methods* **180**(2–3) (1981) 409–412 [https://doi.org/10.1016/0029-554X\(81\)90080-X](https://doi.org/10.1016/0029-554X(81)90080-X)
- [44] M. L. Cherry, *Measuring the Lorentz Factors of Energetic Particles with Transition Radiation*, *Nucl. Instrum. Meth. in Phys. Res. A* **706** (2013) 39–42. <https://doi.org/10.1016/j.nima.2012.05.008>
- [45] M. Albrow et. al., *Transition radiation detectors for hadron separation in the forward direction of LHC experiments*, *NIMA* **1055** (2023) 168535. <https://doi.org/10.1016/j.nima.2023.168535>